The Gluco- and Liporegulatory and Vasodilatory Effects of Glucose-Dependent Insulinotropic Polypeptide (GIP) Are Abolished by an Antagonist of the Human GIP Receptor

Meena Asmar,[1,2] Ali Asmar,[2] Lene Simonsen,[2] Lærke Smidt Gasbjerg,[3,4] Alexander Hovard Sparre-Ulrich,[4] Mette Marie Rosenkilde,[3,4] Bolette Hartmann,[3,4] Flemming Dela,[5,6] Jens Juul Holst,[3,4] and Jens Bülow[2,4]

Diabetes 2017;66:2363–2371 | https://doi.org/10.2337/db17-0480

A truncated form of human glucose-dependent insulinotropic polypeptide (GIP), GIP(3–30)NH_2, was recently identified as an antagonist of the human GIP receptor. This study examined the ability of GIP(3–30)NH_2 to antagonize the physiological actions of GIP in glucose metabolism, subcutaneous abdominal adipose tissue blood flow (ATBF), and lipid metabolism in humans. Eight lean subjects were studied by measuring arteriovenous concentrations of metabolites and ATBF on three different occasions during hyperglycemic-hyperinsulinemic clamps with concomitant infusions of GIP, GIP(3–30)NH_2, or both GIP and GIP(3–30)NH_2. During infusion of GIP(3–30)NH_2 alone and in combination with GIP, insulin levels and the total glucose amount infused to maintain the clamp were lower than during GIP alone. In addition, ATBF remained constant during the antagonist and increased only slightly in combination with GIP, whereas it increased fivefold during GIP alone. Adipose tissue triacylglyceride (TAG) and glucose uptake decreased, and the free fatty acid/glycerol ratio increased during the antagonist alone and in combination with GIP. The changes in glucose infusion rates and plasma insulin levels demonstrate an inhibitory effect of the antagonist on the incretin effect of GIP. In addition, the antagonist inhibited GIP-induced increase in ATBF and decreased the adipose tissue TAG uptake, indicating that GIP also plays a crucial role in lipid metabolism.

Glucose-dependent insulinotropic polypeptide (GIP) is a hormone secreted from the K cells of the gut after a meal. The hormone potentiates glucose-induced insulin secretion and is partly responsible for the incretin effect. Besides enhancing insulin secretion, GIP has been shown to have an effect on human subcutaneous abdominal adipose tissue blood flow (ATBF) and lipid metabolism (1–3).

We have previously demonstrated that GIP infusions in the presence of elevated insulin concentrations increased ATBF and stimulated triacylglyceride (TAG) deposition in adipose tissue in lean humans (1), suggesting that GIP together with insulin are controllers of postprandial fat deposition. In the same study, we showed that GIP alone or hyperinsulinemia per se did not have any effect on ATBF. In a recent study, we showed that insulin is permissive for GIP to induce an increase in ATBF and TAG clearance in subcutaneous abdominal adipose tissue in lean humans (4).

In obese humans with impaired glucose tolerance, GIP infusion in combination with hyperinsulinemia did not induce any changes in ATBF and TAG uptake in subcutaneous abdominal adipose tissue (5). Recently, we showed that weight loss in obese subjects with impaired glucose tolerance induced by caloric restriction resulted in improved insulin sensitivity and partly restored the increase in ATBF during otherwise comparable experimental conditions (6).

These studies suggest that GIP in combination with insulin plays a key role in the regulation of ATBF and lipid deposition. Recently, it was demonstrated that a truncated form of human GIP, GIP(3–30)NH_2, is a high-affinity competitive antagonist of the human GIP receptor in vitro (7) and that it inhibits insulin, glucagon, and somatostatin

[1]Department of Endocrinology, Bispebjerg University Hospital, Copenhagen, Denmark
[2]Department of Clinical Physiology and Nuclear Medicine, Bispebjerg University Hospital, Copenhagen, Denmark
[3]Novo Nordisk Foundation Center for Basic Metabolic Research, University of Copenhagen, Copenhagen, Denmark
[4]Department of Biomedical Sciences, University of Copenhagen, Copenhagen, Denmark
[5]Xlab, Center for Healthy Aging, University of Copenhagen, Copenhagen, Denmark
[6]Department of Geriatrics, Bispebjerg University Hospital, Copenhagen, Denmark

Corresponding author: Meena Asmar, masmar@sund.ku.dk.

Received 21 April 2017 and accepted 20 June 2017.

release in perfused rat pancreas (8). Until now, antagonists of the GIP receptor have not been investigated in humans, but only in animal models, in which, in particular, the rodent models have been troublesome because of substantial differences between the human and rodent GIP systems (9). Thus, our knowledge regarding the physiological role of GIP is based on mimicry studies in which the effects of physiological plasma GIP excursions, brought about by infusions, have been studied. Therefore, this study was designed to assess the ability of GIP(3–30)NH_2 to antagonize the actions of GIP in lean humans. We examined the effects of GIP(3–30)NH_2 on glucose metabolism, subcutaneous ATBF, and lipid metabolism.

RESEARCH DESIGN AND METHODS

Subjects

Eight healthy nonsmoking males (mean age 26 ± 2 years [mean ± SD]; BMI 23.3 ± 1.4 kg/m^2) were studied. Sample size was determined before the study using power analysis (P = 0.8; α = 0.05) with regard to ATBF response based on our previous publications (1,4). Assuming an ATBF response as found in normal-weight, healthy subjects, less than six subjects were needed in the current study.

None of them used medication or had a positive family history of diabetes. All volunteers had normal plasma values of fasting glucose, hemoglobin, lipid profile, and renal and hepatic function. All subjects gave informed written consent to participate. The protocol was approved by the ethical committee of Copenhagen Municipality (H-15013961), and the study was performed in accordance with the Helsinki Declaration II.

Experimental Design

The study protocol had a crossover design with a washout period of at least 2 weeks. Each subject served as his own control and was studied, in a randomized order, on three different occasions during infusion of: *1*) GIP (1.5 pmol/kg/min); *2*) GIP(3–30)NH_2 (1,000 pmol/kg/min); and *3*) GIP and GIP(3–30)NH_2 during 120 min—all 3 days in combination with hyperglycemic-hyperinsulinemic (Hy_{gluc}-Hy_{insu}) clamps, raising plasma glucose and insulin to postprandial levels.

Protocol

The subjects were instructed to abstain from drinking alcohol or doing strenuous physical activities for 2 days before the experiments to ensure equally filled glycogen stores. On the days of the experiments, subjects arrived at the department at 8:00 A.M. having used nonstrenuous transportation and having fasted for at least 12 h. The investigations were performed with the subjects in supine position in a room kept at 24°C. A catheter (BD Venflon Pro; BD Biosciences, Singapore) was inserted into an antecubital vein for the infusion of GIP, GIP(3–30)NH_2, glucose, and insulin. The subjects then had catheters inserted into a subcutaneous vein in the anterior abdominal wall and into a radial artery.

Catheterization

A vein draining the subcutaneous abdominal adipose tissue in the anterior abdominal wall was catheterized antegradely as previously described (10) during ultrasound/color-Doppler imaging of the vein. A 22-gauge, 10-cm polyurethane catheter (Ohmeda, Swindon, U.K.) was inserted using the Seldinger technique. The tip of the catheter was positioned above the inguinal ligament to minimize the risk of withdrawing blood from the femoral vein. After insertion, the catheter was kept patent throughout the experiment by continuous infusion of saline at a rate of 40 mL h^{-1}. Another catheter was inserted percutaneously into the radial artery of the nondominant arm under local analgesia (1 mL 1% lidocaine) with an Artflon (Ohmeda). The catheter was kept patent with regular flushing with saline.

After baseline measurements (time −30, −15, and 0 min), a continuous infusion of GIP, GIP(3–30)NH_2, or GIP and GIP(3–30)NH_2 in combination with the clamp was started.

GIP and GIP(3–30)NH_2 Infusions and the Clamp

GIP and GIP(3–30)NH_2

Synthetic human GIP(1–42) was purchased from Bachem (Bubendorf, Switzerland) and demonstrated to be >97% pure and identical to the natural human peptide by high-performance liquid chromatography, mass, and sequence analysis. GIP(1–42) was dissolved in saline containing 0.5% human serum albumin (human albumin; CSL Behring, Marburg, Germany) and subjected to sterile filtration. GIP(3–30)NH_2 (purity 98%) was purchased from Caslo (Kongens Lyngby, Denmark) and dissolved in a sodium hydrogen carbonate buffer with 0.5% human serum albumin. Appropriate amounts of peptides for each experimental subject were dispensed into glass ampoules and stored frozen (−20°C) until the day of the experiment. Vial content was tested for sterility and bacterial endotoxins (European Pharmacopoeia 2.6.14, Method C. Turbidimetric kinetic method).

Hy_{gluc}-Hy_{insu} Clamp

The objective of the Hy_{gluc}-Hy_{insu} clamp was to increase plasma glucose levels above fasting levels (6.5–7 mmol/L) and increase insulin concentration to physiological postprandial levels. The protocol included: *1*) a continuous variable glucose infusion dose was adjusted every 5–10 min according to measured plasma glucose to maintain the glucose concentration at the desired target; and *2*) a continuous infusion of insulin (Actrapid Human; Novo Nordisk, Copenhagen, Denmark) at a rate of 7 mU m^{-2} min^{-1} was infused to raise plasma insulin levels to postprandial levels.

Measurements

ATBF

ATBF measurements were performed for the duration of each experiment by recording washout of ^{133}Xe, which was injected in gaseous form into the adipose tissue. This technique has previously been validated in our laboratory

(11). Approximately 1 MBq gaseous ^{133}Xe (The Hevesy Laboratory, Risoe National Laboratory, Roskilde, Denmark) mixed in ~0.1 mL atmospheric air was injected into the paraumbilical area of the subcutaneous adipose tissue. The washout rate of ^{133}Xe was measured continuously by a scintillation-counting device placed over the exact site of injection and taped firmly in place (Mediscint; Oakfield Instruments, Oxford, U.K.). The ATBF was calculated from the mean washout rate constant determined in 30-min periods corresponding to the time points when blood samples were drawn. A tissue/blood partition coefficient for xenon of 10 mL g^{-1} was used. To detect early flow changes, a monoexponential curve was fitted to the washout curve registered in the basal control period immediately before the hormone infusions were initiated. The commencement of the vascular effects was defined when the slope of the xenon-washout curve deviated from the baseline slope by visual inspection.

Blood Samples

Blood samples were drawn at time −30, −15, and 0 min and thereafter every 30 min until discontinuation of the infusion. Plasma glucose concentrations were measured every 5–10 min for clamp adjustments. Blood samples were drawn simultaneously from the two catheters (arterial and adipose tissue) for measurements of TAG, glycerol, free fatty acids (FFA), and glucose. In addition, blood samples were collected from the artery for measurements of GIP, GIP(3–30)NH_2, insulin, and C-peptide. Blood samples were collected into iced chilled tubes (Vacuette; Greiner Bio-One, Kremsmünster, Austria). Tubes for total GIP contained EDTA and a specific dipeptidyl peptidase 4 inhibitor, and tubes for insulin and C-peptide contained heparin. Tubes for glucose, TAG, FFA, and glycerol contained EDTA. All samples were centrifuged within 15 min for 15 min at 5,000*g* at 4°C and stored at −80°C until analysis.

Blood Analysis

Total GIP was measured using a C-terminally directed antibody (code number 80867), which reacts fully with intact GIP and N-terminally truncated forms as described in Lindgren et al. (12). The standard was human GIP (H-5645; Bachem), and the tracer was ^{125}I-labeled human GIP (Nex402; PerkinElmer).

GIP(3–30)NH_2 was measured using an antibody directed against the COOH-terminal part of GIP (1–30)NH_2 (code number 95234). As a standard, we used human GIP(1–30)NH_2 (027–30; Phoenix Pharmaceuticals), and the tracer was ^{125}I-labeled human GIP.

Plasma glucose (Glucose/HK; Roche Diagnostics, Mannheim, Germany), TAG (Triglyceride GPO-PAP; Roche Diagnostics), FFA (NEFA C kit; Wako Chemicals, Neuss, Germany), and glycerol (Boehringer Mannheim, Mannheim, Germany) were measured by enzymatic methods modified to run on a COBAS 6000 automatic analyzer (Roche, Rødovre, Denmark).

Plasma insulin and C-peptide concentrations were measured by AutoDELFIA automatic fluoroimmunoassay (Wallac, Inc., Turku, Finland).

Plasma glucose was measured bedside during the clamp experiments using an ABL 725 blood gas analyzer (Radiometer Corp., Brønshøj, Denmark).

Calculations and Statistical Analysis

The ATBF (adipose tissue perfusion coefficient) was calculated from the mean washout rate constant determined in 30-min periods corresponding to the time points when blood samples were drawn. ATBF was then calculated according to the equation ATBF = $-k \times \lambda \times 100$, where k is the xenon washout constant, and λ is the tissue/blood partition coefficient for xenon (13).

Subcutaneous abdominal adipose tissue metabolic net fluxes were calculated by multiplication of the arteriovenous or venoarterial concentration differences of the metabolites and the appropriate flow value (whole blood for calculation of glycerol and glucose fluxes [14] and plasma flow for calculation of fatty acid and TAG fluxes).

Adipose tissue is a major site of clearance of postprandial lipemia through the action of lipoprotein lipase (LPL) (15). The FFA released by LPL from circulating TAG is directed into the tissue for esterification and storage. However, some of the fatty acids may also be released to the systemic circulation. FFA released by the action of hormone-sensitive lipase (HSL) in the adipocytes in the fasting state is mainly released into the circulation (15). Regulation of FFA release from the adipose tissue depends on coordinated activities in HSL and LPL. Calculations of the relative rates of action of HSL and LPL can be done as described in Frayn et al. (16). The calculations are as follows:

$$\text{LPL action} = (\text{A-V})_{\text{TAG(glycerol concentrations units)}}$$

$$\text{HSL action} = (\text{V-A})_{\text{glycerol}} - \text{LPL action}_{\text{(glycerol concentration units)}}$$

Overall re-esterification of fatty acids within the tissue was calculated on the assumption that hydrolysis of TAG releases one glycerol and three fatty acids, as:

$$\text{Overall tissue reesterification}(\% \text{ of fatty acids released}) = \left(1 - \left((\text{V-A})_{\text{FFA}}/3\right) \times \left((\text{V-A})_{\text{glycerol}}\right)\right) \times 100$$

All results are presented as mean ± SEM. Areas under the curve were calculated using the trapezoidal rule and are presented as the incremental values. The significance of changes in ATBF and arterial hormone with time was evaluated using two-way ANOVA for repeated measures. Significant differences in ATBF areas under the curve and metabolite fluxes were evaluated by paired t test. The P values <0.05 were considered statistically significant.

Table 1—GIP(1–42) and GIP(3–30)NH_2 plasma concentrations

Infusions	Basal (−30 to 0 min)	Steady state (30–120 min)
Total GIP(1–42) concentrations (pmol/L)		
GIP(1–42)	8.8 ± 0.6	111.2 ± 10.9
GIP(3–30)NH_2	11.2 ± 0.6	7.9 ± 0.4
GIP(1–42) + GIP(3–30)NH_2	10.3 ± 0.5	117.3 ± 13.7
GIP(3–30)NH_2 concentrations (nmol/L)		
GIP(1–42)	0.7 ± 0.1	0.9 ± 0.1
GIP(3–30)NH_2	0.2 ± 0.1	66.4 ± 10.7
GIP(1–42) + GIP(3–30)NH_2	0.9 ± 0.1	68.3 ± 10.6

Data are shown as mean ± SEM.

RESULTS

Arterial Hormone and Glucose Concentrations

Total plasma GIP concentrations increased significantly from fasting levels and after ~30 min reached mean plateau levels of 111.2 ± 10.9 pmol/L during infusion of GIP and 117.3 ± 13.7 pmol/L during infusion of both GIP and GIP(3–30)NH_2 (Table 1) ($P < 0.001$). Plasma GIP(3–30)NH_2 concentrations increased likewise significantly from fasting levels and reached mean plateau levels of 66.2 ± 10.7 nmol/L after ~30 min of infusion and 68.3 ± 10.6 nmol/L during infusion of both GIP and GIP(3–30)NH_2 (Table 1) ($P < 0.001$).

The clamps were carried out successfully. Plasma glucose levels reached the target levels of 6.8 ± 0.1, 6.9 ± 0.04, and 6.8 ± 0.03 mmol/L 30 min after start of the infusion of GIP, GIP and GIP(3–30)NH_2, or GIP(3–30)NH_2, respectively (Fig. 1*A*). The total amount of glucose infused was significantly higher during infusion of GIP alone compared with infusion of GIP(3–30)NH_2 alone or a combination of GIP and GIP(3–30)NH_2 (Fig. 1*B*) ($P = 0.01$), reflecting different insulin concentrations during the three experiments. The amount of glucose infused during the antagonist and both ligands were similar. During infusion of GIP, plasma insulin levels increased after 30 min and reached target levels of 396 ± 6 pmol/L (Fig. 1*C*) and were higher ($P < 0.0001$) than the insulin levels 30 min after infusion of GIP (3–30)NH_2 and both ligands (205 ± 6 and 257 ± 8 pmol/L, respectively) (Fig. 1*C*). During infusion of both GIP and GIP (3–30)NH_2, the insulin levels were slightly higher between 20 and 90 min ($P = 0.01$) compared with insulin levels during the GIP(3–30)NH_2 alone ($P = 0.01$).

C-peptide levels increased significantly after 30 min during infusion of GIP and were significantly higher (1,619 ± 104 pmol/L) than the levels of C-peptide during infusion of GIP(3–30)NH_2 (948 ± 62 pmol/L) and of both GIP and GIP(3–30)NH_2 (942 ± 49 pmol/L) (Fig. 1*D*) ($P < 0.001$). During the last two infusions, C-peptide levels did not increase and were almost similar.

The arterial concentrations of the metabolites are given in Fig. 2. Arterial TAG concentrations were similar during

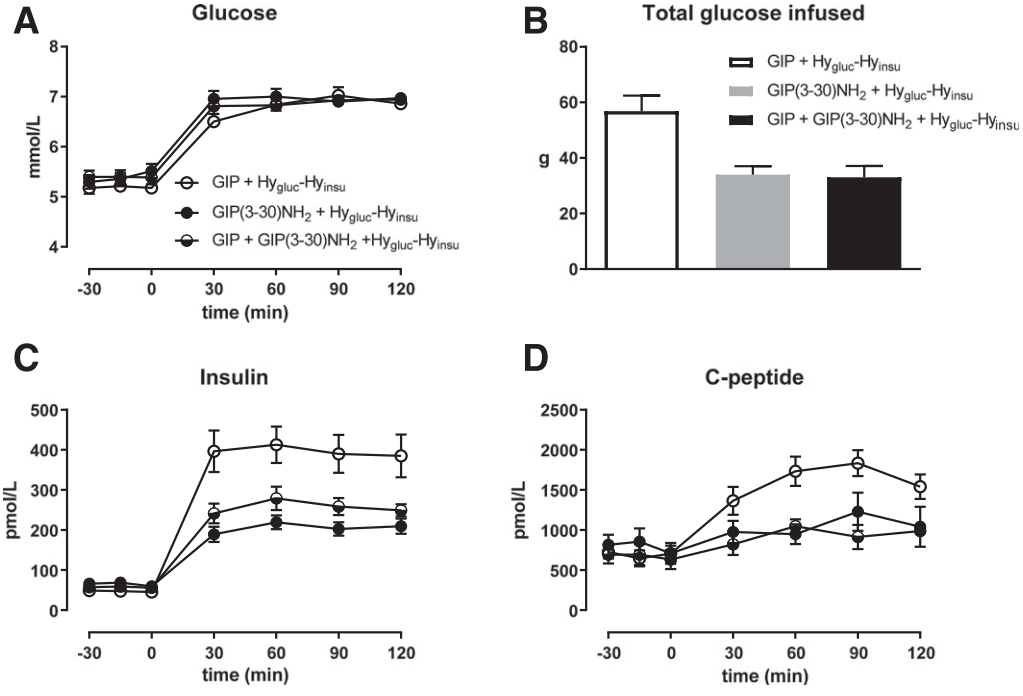

Figure 1—Plasma arterial glucose (*A*), insulin (*C*), and C-peptide (*D*) concentrations during GIP infusion in combination with Hy_{gluc}-Hy_{insu} clamp, GIP(3–30)NH_2 with Hy_{gluc}-Hy_{insu} clamp, and GIP in combination with GIP(3–30)NH_2 and Hy_{gluc}-Hy_{insu} clamp. Bar graph in *B* shows total amount of glucose infused during GIP, GIP(3–30)NH_2, and both GIP and GIP(3–30)NH_2 all 3 days in combination with Hy_{gluc}-Hy_{insu} clamp. Data are mean ± SEM.

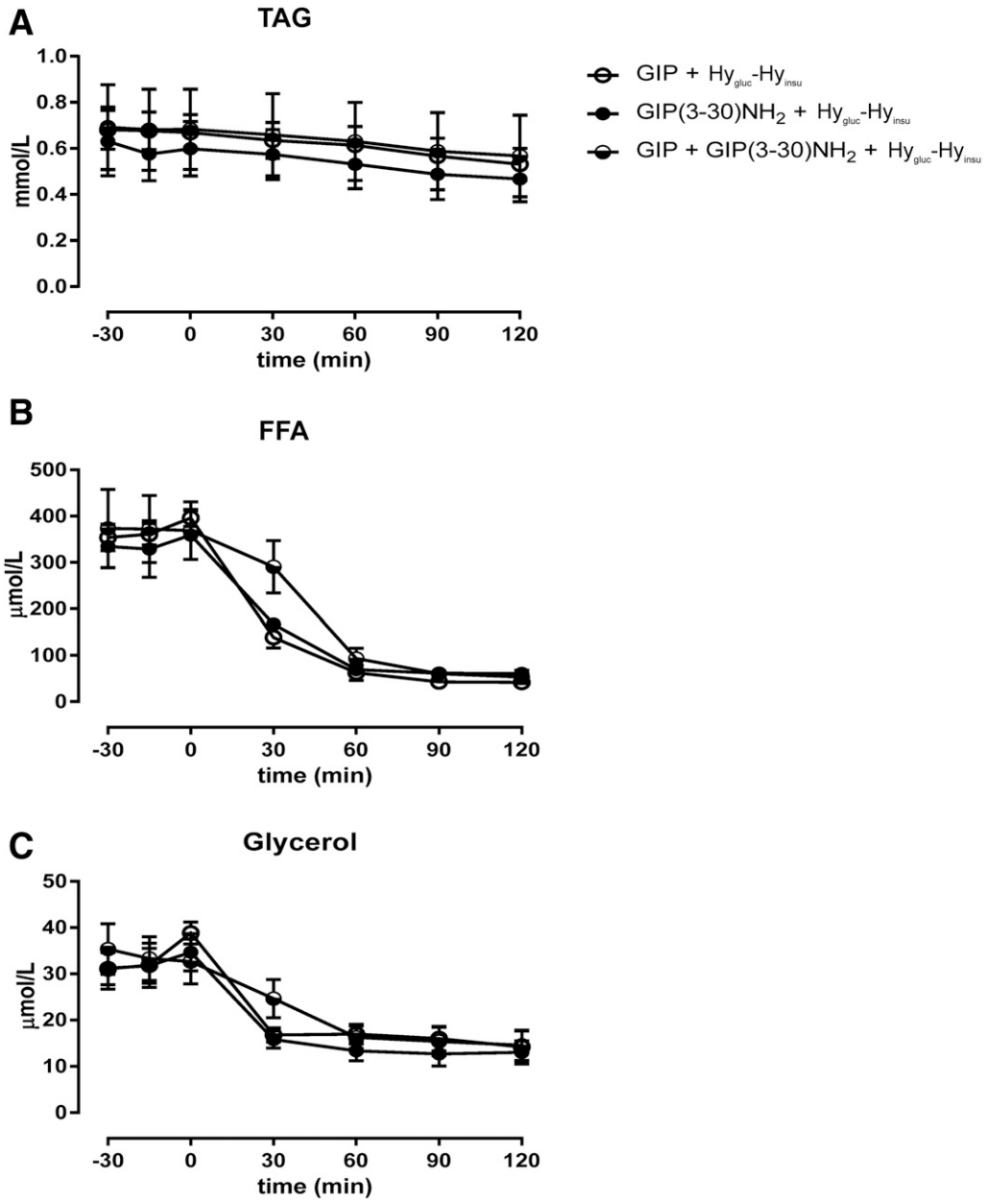

Figure 2—Plasma arterial TAG (*A*), FFA (*B*), and glycerol (*C*) concentrations during GIP infusion in combination with Hy_{gluc}-Hy_{insu} clamp, GIP(3–30)NH_2 with Hy_{gluc}-Hy_{insu} clamp, and GIP in combination with GIP(3–30)NH_2 and Hy_{gluc}-Hy_{insu} clamp. Data are mean ± SEM.

the three experiments and exhibited a slight decrease toward the end of the study (Fig. 2*A*). Arterial FFA and glycerol concentrations decreased significantly (P = 0.02), with no differences seen among the three experiments (Fig. 2*B* and *C*).

Changes in Subcutaneous Abdominal ATBF

Figure 3 shows the subcutaneous abdominal ATBF during the three experiments. Baseline ATBF did not differ among the three study days (2.6 ± 0.6, 2.5 ± 0.5 and 2.4 ± 0.5 mL min^{-1} 100 g $tissue^{-1}$). During the antagonist GIP(3–30)NH_2, ATBF remained constant throughout the experiment (2.8 ± 0.1 mL min^{-1} 100 g $tissue^{-1}$), whereas ATBF increased almost fivefold during GIP (13.7 ± 0.7 mL min^{-1} 100 g $tissue^{-1}$; P = 0.004). During infusion of both GIP and GIP(3–30)NH_2, ATBF increased only slightly (5.1 ± 0.4 mL min^{-1} 100 g $tissue^{-1}$; P = 0.02).

Changes in Net Fluxes of TAG, FFA, Glycerol, and Glucose and the Action of the Enzymes LPL and HSL

Figure 4 shows net fluxes of TAG, FFA, glycerol, and glucose in adipose tissue. Baseline TAG, FFA, glycerol, and glucose fluxes were similar during the three experiments (Fig. 4*A*, *C*, *E*, and *G*). During GIP infusion, TAG clearance increased ($P < 0.001$) (Fig. 4*B*) and glucose uptake

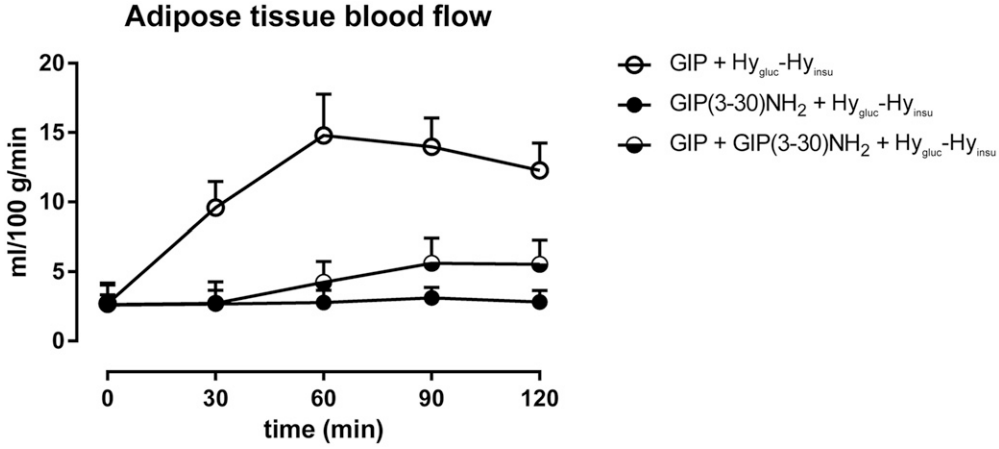

Figure 3—Absolute ATBF during GIP infusion in combination with Hy_{gluc}-Hy_{insu} clamp and GIP(3–30)NH_2 with Hy_{gluc}-Hy_{insu} clamp and during GIP infusion in combination with GIP(3–30)NH_2 and Hy_{gluc}-Hy_{insu} clamp. Data are mean ± SEM.

increased ($P < 0.001$) (Fig. 4*H*), whereas FFA output (Fig. 4*D*) and FFA/glycerol ratio (Fig. 4*J*) decreased ($P = 0.02$) compared with GIP(3–30)NH_2 alone and GIP(3–30)NH_2 in combination with GIP. The glycerol levels were not affected by the two ligands alone or in combination (Fig. 4*F*).

The actions of the enzymes LPL and HSL and the overall re-esterification are given in Table 2. As expected, during baseline (fasting state), the action of HSL was high, indicating that there was net outward flux of FFA, and therefore, the overall re-esterification was low. During the infusions of the ligands, the action of HSL fell. LPL action increased significantly during GIP and the clamp. There was an increase in overall re-esterification, indicating that the major proportion of LPL-derived FFA is directed into the adipose tissue for re-esterification and storage. The GIP antagonist reduced this re-esterification approximately threefold.

DISCUSSION

This present study clearly demonstrates GIP(3–30)NH_2 as an effective antagonist of GIP in vivo in humans. The main findings of the current study are that GIP(3–30)NH_2: *1*) inhibits the insulinotropic effects of GIP; and *2*) antagonizes the liporegulatory and vasodilatory effects of GIP. On the basis of these results, we propose the use of GIP (3–30)NH_2 as a new tool to characterize the significance of endogenous GIP in the regulation of glucose and lipid metabolism in humans.

Recently, a study with cells expressing the human GIP receptor showed that GIP(3–30)NH_2 bound with high affinity to the GIP receptor (K_d 3.4 nmol/L) (i.e., only a fivefold lower affinity compared with human GIP [1–42]) (K_d 0.67 nmol/L) was able to inhibit GIP-induced cAMP accumulation (7), thus demonstrating GIP(3–30)NH_2 as a potent and efficacious antagonist for the human GIP receptor with competitive properties. Similarly, a study in the rat showed that rat GIP(3–30)NH_2 potently and efficaciously inhibited cAMP production from the rat GIP receptor in vitro and inhibited GIP-induced insulin, glucagon, and somatostatin release in perfused rat pancreas (8). The dose of GIP(3–30)NH_2 infused in the current study was derived from the earlier study in the human GIP system (7) showing that a 100-fold excess of the antagonist in relation to GIP dose would completely block the action of GIP in vitro. However, one can speculate whether a lower dose of GIP(3–30)NH_2 would have been sufficient in vivo. The intravenous infusions of GIP(3–30)NH_2 were well tolerated in all volunteers. Physiological postprandial plasma levels of GIP were reached with the chosen dose of GIP. Likewise, we managed to mimic normal postprandial plasma glucose and insulin levels during the Hy_{gluc}-Hy_{insu} clamp. In this context, in spite of the clamp, the insulin levels were clearly elevated by GIP, and this also resulted in a higher amount of glucose required to maintain the clamp. However, during the coinfusion of GIP(3–30)NH_2 and GIP, the required amount of glucose to maintain the clamp was significantly lower. This presumably reflects the antagonist's effect on GIP-stimulated insulin secretion. In parallel, the endogenous C-peptide levels were inhibited during GIP (3–30)NH_2 alone and in combination with GIP, illustrating the extensive antagonistic effect of GIP(3–30)NH_2 on the β-cells. The effect observed in this study is in agreement with results from a recent human study (L.S. Gasberg, unpublished observations) and results from previous studies in rodents in which GIP(3–30)NH_2, GIP (7–30)NH_2, or GIP receptor antibodies, demonstrated to have antagonistic properties, decreased GIP-stimulated insulin secretion in vivo (8,17,18). Surprisingly, the levels of insulin were higher during infusion of both GIP(3–30)NH_2 and GIP compared with GIP(3–30)NH_2 alone despite the fact that the C-peptide levels were similar and the same rate of insulin was infused on both days. These results suggest that GIP may have a reducing effect on the hepatic insulin clearance; however, this is in contrast to previous findings (19,20).

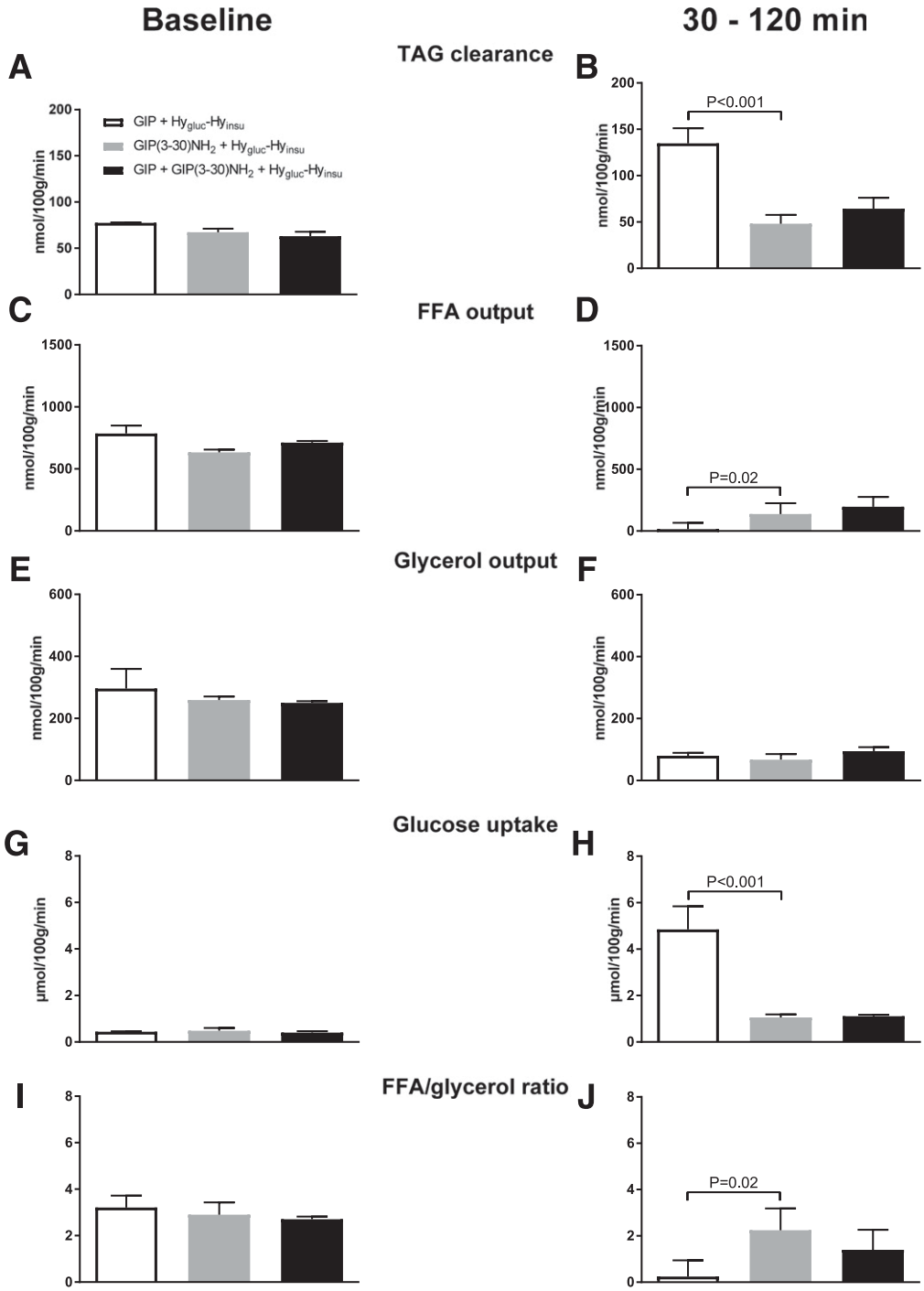

Figure 4—Average net fluxes of TAG, FFA, glycerol, and glucose in subcutaneous abdominal adipose tissue during the preinfusion baseline period (*A*, *C*, *E*, and *G*) and in the steady-state period from 30–120 min (*B*, *D*, *F*, and *H*) after commencement of the infusions. Average adipose tissue FFA/glycerol output ratio during the preinfusion baseline period (*I*) and in the period from 30–120 min (*J*) after commencement of infusions. Data are mean ± SEM.

ATBF increases significantly postprandially, and this increase seems to be of particular importance in the regulation of lipid metabolism by facilitating transport and deposition of lipids in adipose tissue (15). The mechanisms by which ATBF is regulated in the postprandial period have been studied in some detail. There are many possible regulators of ATBF, including neural and endocrine systems (1,21–24). ATBF might be regulated by more than one system at any one time. In humans, adrenergic influences are predominant, with β-mediated vasodilatation (21,24) and α2-mediated vasoconstriction (25). These influences may explain the increased blood flow during fasting or exercise.

Table 2—Actions of enzymes LPL and HSL and overall re-esterification

	LPL action	HSL action	Overall re-esterification (%)
Baseline			
GIP	77 ± 1	219 ± 15	11
GIP(3–30)NH_2	67 ± 4	192 ± 12	19
GIP + GIP(3–30)NH_2	63 ± 5	187 ± 6	15
30–120 min			
GIP	135 ± 11	−54 ± 10	94
GIP(3–30)NH_2	58 ± 10	19 ± 13	32
GIP + GIP(3–30) NH_2	64 ± 12	31 ± 13	31

Data are shown as mean ± SEM.

The increase in blood flow after food intake parallels that of plasma GIP and insulin concentrations (26). In agreement with our previous studies (1,4), infusion of GIP during a Hy_{gluc}-Hy_{insu} clamp increased ATBF almost fivefold. During infusion of the GIP receptor antagonist, GIP(3–30)NH_2, ATBF remained constant throughout the experiment, indicating that GIP has crucial vasoactive effects in adipose tissue. In the presence of both GIP and GIP(3–30)NH_2, ATBF increased only slightly, again attesting to the powerful antagonistic properties of the antagonist. The incomplete suppression is consistent with the incomplete suppression of GIP-induced insulin secretion and our recent demonstration that insulin plays a permissive role in the GIP-induced vasodilation in adipose tissue (4). Concomitantly with the increase in ATBF during infusion of GIP under clamp conditions, an increase in adipose tissue TAG clearance took place, in agreement with our previous findings (1,4), reflecting an increased substrate supply to LPL similar to that seen after a mixed meal (27). Simultaneously with the GIP-induced increased TAG clearance, an increase in adipose tissue glucose uptake took place, and there was a decrease in the ratio of glycerol to FFA release. This ratio can be used to estimate the extent of in situ FFA re-esterification. A ratio of approximately three indicates that the fatty acids derived from intracellular lipolysis are released into the circulation, whereas a ratio of approximately zero indicates that the fatty acids are completely re-esterified in situ and stored as TAG again (28). These changes were confirmed by calculations of the LPL activity and re-esterification, which were high during GIP, indicating increased adipose tissue TAG deposition. This process was strongly inhibited by the GIP(3–30)NH_2 infusion. Previous in vitro and animal studies have shown that GIP may play a role in obesity and have suggested that GIP receptor may represent a target for the prevention and treatment of obesity (29,30). The present results clearly demonstrate that the GIP-induced deposition of fat in abdominal subcutaneous adipose tissue can be prevented by a GIP receptor antagonist.

In conclusion, during administration of the GIP receptor antagonist, subcutaneous abdominal ATBF remained unchanged, whereas the TAG uptake in this adipose tissue depot decreased compared with GIP and insulin, indicating that GIP together with insulin plays a crucial role in adipose tissue lipid metabolism. Furthermore, the antagonist inhibited the insulinotropic effect of GIP.

Acknowledgments. The authors thank Bente Matthiesen (Department of Clinical Physiology and Nuclear Medicine, Bispebjerg University Hospital, Copenhagen, Denmark) for technical assistance.

Funding. This study was supported by a European Foundation for the Study of Diabetes research grant and Novo Nordisk Foundation.

Duality of Interest. No potential conflicts of interest relevant to this article were reported.

Author Contributions. M.A. designed the study, recruited the subjects, supervised the studies, collected and analyzed the data, and wrote the manuscript. A.A. recruited the subjects, supervised the studies, collected and analyzed the data, and reviewed and edited the manuscript. L.S. supervised the studies and reviewed and edited the manuscript. L.S.G., A.H.S.-U., M.M.R., B.H., and J.J.H. contributed to the formulation of the antagonist, analyzed the samples, and reviewed the manuscript. F.D. analyzed the samples and reviewed the manuscript. J.B. designed the study, supervised the studies, and reviewed and edited the manuscript. M.A., A.A., J.J.H., and J.B. are the guarantors of this work and, as such, had full access to all of the data in the study and take responsibility for the integrity of the data and the accuracy of the data analysis.

Prior Presentation. Parts of this study were presented in poster form at the 77th Scientific Sessions of the American Diabetes Association, San Diego, CA, 9–13 June 2017.

References

1. Asmar M, Simonsen L, Madsbad S, Stallknecht B, Holst JJ, Bülow J. Glucose-dependent insulinotropic polypeptide may enhance fatty acid re-esterification in subcutaneous abdominal adipose tissue in lean humans. Diabetes 2010;59:2160–2163

2. Asmar M, Tangaa W, Madsbad S, et al. On the role of glucose-dependent insulintropic polypeptide in postprandial metabolism in humans. Am J Physiol Endocrinol Metab 2010;298:E614–E621

3. Holst JJ, Windeløv JA, Boer GA, et al. Searching for the physiological role of glucose-dependent insulinotropic polypeptide. J Diabetes Investig 2016;7(Suppl. 1): 8–12

4. Asmar M, Simonsen L, Asmar A, Holst JJ, Dela F, Bülow J. Insulin plays a permissive role for the vasoactive effect of GIP regulating adipose tissue metabolism in humans. J Clin Endocrinol Metab 2016;101:3155–3162

5. Asmar M, Simonsen L, Arngrim N, Holst JJ, Dela F, Bülow J. Glucose-dependent insulinotropic polypeptide has impaired effect on abdominal, subcutaneous adipose tissue metabolism in obese subjects. Int J Obes 2014;38:259–265

6. Asmar M, Arngrim N, Simonsen L, et al. The blunted effect of glucose-dependent insulinotropic polypeptide in subcutaneous abdominal adipose tissue in obese subjects is partly reversed by weight loss. Nutr Diabetes 2016;6:e208

7. Hansen LS, Sparre-Ulrich AH, Christensen M, et al. N-terminally and C-terminally truncated forms of glucose-dependent insulinotropic polypeptide are high-affinity competitive antagonists of the human GIP receptor. Br J Pharmacol 2016;173:826–838

8. Sparre-Ulrich AH, Gabe MN, Gasbjerg LS, et al. GIP(3-30)NH2 is a potent competitive antagonist of the GIP receptor and effectively inhibits GIP-mediated insulin, glucagon, and somatostatin release. Biochem Pharmacol 2017; 131:78–88

9. Sparre-Ulrich AH, Hansen LS, Svendsen B, et al. Species-specific action of (Pro3)GIP - a full agonist at human GIP receptors, but a partial agonist and competitive antagonist at rat and mouse GIP receptors. Br J Pharmacol 2016;173:27–38

10. Simonsen L, Bülow J, Madsen J. Adipose tissue metabolism in humans determined by vein catheterization and microdialysis techniques. Am J Physiol 1994; 266:E357–E365

11. Simonsen L, Enevoldsen LH, Bülow J. Determination of adipose tissue blood flow with local ^{133}Xe clearance. Evaluation of a new labelling technique. Clin Physiol Funct Imaging 2003;23:320–323

12. Lindgren O, Carr RD, Deacon CF, et al. Incretin hormone and insulin responses to oral versus intravenous lipid administration in humans. J Clin Endocrinol Metab 2011;96:2519–2524
13. Bülow J, Jelnes R, Astrup A, Madsen J, Vilmann P. Tissue/blood partition coefficients for xenon in various adipose tissue depots in man. Scand J Clin Lab Invest 1987;47:1–3
14. Bülow J, Madsen J. Influence of blood flow on fatty acid mobilization form lipolytically active adipose tissue. Pflugers Arch 1981;390:169–174
15. Frayn KN. Adipose tissue as a buffer for daily lipid flux. Diabetologia 2002;45: 1201–1210
16. Frayn KN, Shadid S, Hamlani R, et al. Regulation of fatty acid movement in human adipose tissue in the postabsorptive-to-postprandial transition. Am J Physiol 1994;266:E308–E317
17. Ravn P, Madhurantakam C, Kunze S, et al. Structural and pharmacological characterization of novel potent and selective monoclonal antibody antagonists of glucose-dependent insulinotropic polypeptide receptor. J Biol Chem 2013;288: 19760–19772
18. Tseng CC, Kieffer TJ, Jarboe LA, Usdin TB, Wolfe MM. Postprandial stimulation of insulin release by glucose-dependent insulinotropic polypeptide (GIP). Effect of a specific glucose-dependent insulinotropic polypeptide receptor antagonist in the rat. J Clin Invest 1996;98:2440–2445
19. Meier JJ, Gallwitz B, Siepmann N, et al. Gastric inhibitory polypeptide (GIP) dose-dependently stimulates glucagon secretion in healthy human subjects at euglycaemia. Diabetologia 2003;46:798–801
20. Meier JJ, Holst JJ, Schmidt WE, Nauck MA. Reduction of hepatic insulin clearance after oral glucose ingestion is not mediated by glucagon-like peptide 1 or gastric inhibitory polypeptide in humans. Am J Physiol Endocrinol Metab 2007;293: E849–E856
21. Ardilouze JL, Fielding BA, Currie JM, Frayn KN, Karpe F. Nitric oxide and beta-adrenergic stimulation are major regulators of preprandial and postprandial subcutaneous adipose tissue blood flow in humans. Circulation 2004;109:47–52
22. Frayn KN, Karpe F. Regulation of human subcutaneous adipose tissue blood flow. Int J Obes 2014;38:1019–1026
23. Patel JN, Eisenhofer G, Coppack SW, Miles JM. Norepinephrine spillover in forearm and subcutaneous adipose tissue before and after eating. J Clin Endocrinol Metab 1999;84:2815–2819
24. Simonsen L, Bülow J, Astrup A, Madsen J, Christensen NJ. Diet-induced changes in subcutaneous adipose tissue blood flow in man: effect of beta-adrenoceptor inhibition. Acta Physiol Scand 1990;139:341–346
25. Hjemdahl P, Akerstedt T, Pollare T, Gillberg M. Influence of beta-adrenoceptor blockade by metoprolol and propranolol on plasma concentrations and effects of noradrenaline and adrenaline during i.v. infusion. Acta Physiol Scand Suppl 1983; 515:45–53
26. Summers LK, Samra JS, Humphreys SM, Morris RJ, Frayn KN. Subcutaneous abdominal adipose tissue blood flow: variation within and between subjects and relationship to obesity. Clin Sci (Lond) 1996;91:679–683
27. Summers LK, Arner P, Ilic V, Clark ML, Humphreys SM, Frayn KN. Adipose tissue metabolism in the postprandial period: microdialysis and arteriovenous techniques compared. Am J Physiol 1998;274:E651–E655
28. Van Hall G, Bülow J, Sacchetti M, Al Mulla N, Lyngso D, Simonsen L. Regional fat metabolism in human splanchnic and adipose tissues; the effect of exercise. J Physiol 2002;543:1033–1046
29. Miyawaki K, Yamada Y, Ban N, et al. Inhibition of gastric inhibitory polypeptide signaling prevents obesity. Nat Med 2002;8:738–742
30. Yamada Y, Seino Y. Physiology of GIP–a lesson from GIP receptor knockout mice. Horm Metab Res 2004;36:771–774